Cell Reports, Volume *42*

Supplemental information

Complex regulation of *Eomes* levels mediated through distinct functional features of the *Meteor* long non-coding RNA locus

Noa Gil, Rotem Ben-Tov Perry, Zohar Mukamel, Alex Tuck, Marc Bühler, and Igor Ulitsky

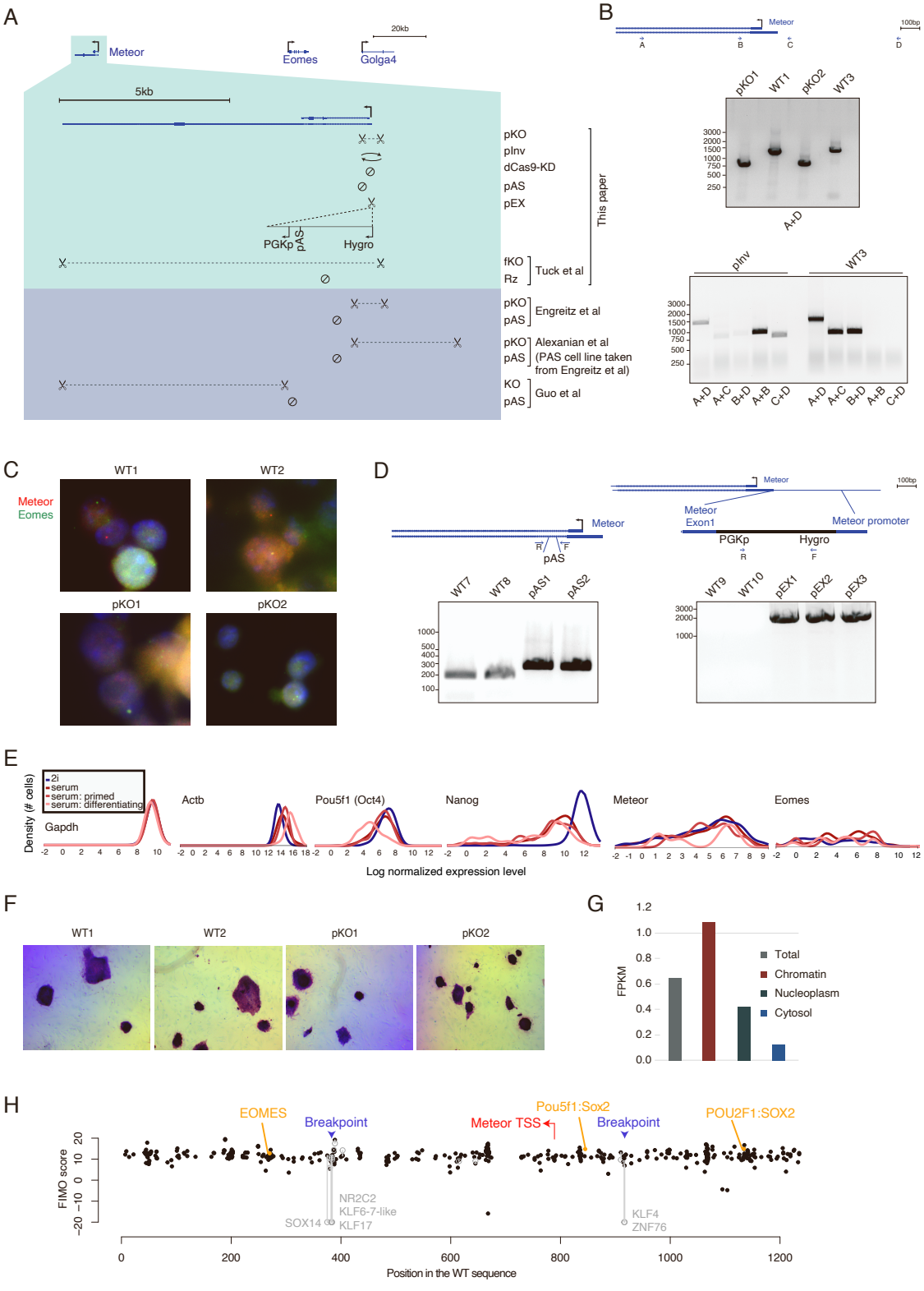
A
Meteor
Eomes
Golga4
20kb
5kb
PGKp
pAS
Hygro
pKO
pInv
dCas9-KD
pAS
pEX
fKO
Rz
Tuck et al
This paper
pKO
pAS
Engreitz et al
pKO
pAS
Alexanian et al
(PAS cell line taken
from Engreitz et al)
KO
pAS
Guo et al
B
Meteor
100bp
A
B
C
D
pKO1
WT1
pKO2
WT3
3000
2000
1500
1000
750
500
250
A+D
pInv
WT3
A+D
A+C
B+D
A+B
C+D
C
WT1
WT2
Meteor
Eomes
pKO1
pKO2
D
Meteor
100bp
Meteor
Exon1
Meteor promoter
Meteor
PGKp
Hygro
pAS
R
F
WT7
WT8
pAS1
pAS2
1000
500
400
300
200
100
WT9
WT10
pEX1
pEX2
pEX3
3000
2000
1000
E
2i
serum
serum: primed
serum: differentiating
Density (# cells)
Gapdh
Actb
Pou5f1 (Oct4)
Nanog
Meteor
Eomes
Log normalized expression level
F
WT1
WT2
pKO1
pKO2
G
FPKM
1.2
1.0
0.8
0.6
0.4
0.2
0.0
Total
Chromatin
Nucleoplasm
Cytosol
H
EOMES
Breakpoint
Meteor TSS
Pou5f1:Sox2
Breakpoint
POU2F1:SOX2
FIMO score
20
10
0
−10
−20
NR2C2
KLF6-7-like
KLF17
SOX14
KLF4
ZNF76
0
200
400
600
800
1000
1200
Position in the WT sequence

Figure S1. Perturbations to the *Meteor* locus. Related to Figure 1.

A. (Top) same as Figure 1A, and (bottom) additional genomic perturbations described in the indicated papers [S1–4] for deleting regions in the *Meteor* locus (KO) or introducing polyadenylation sites (pAS). **B.** Schematic locations and directionalities of the primers used to probe genomic deletions in the *Meteor* locus (top), and the resulting PCR products (bottom). PCR was performed on the indicated cell lines using the primers indicated below the blots (see **Method Details** and **Table S1**). PCR using primers B and C was performed on DNA pre-amplified with primers A and D. **C.** Single molecule FISH using probes against *Meteor* (red) and *Eomes* (green) as well as DAPI staining (blue) in WT and *Meteor* pKO cells grown in 2i conditions, imaged using 100X objectives. No *Meteor* signal was detected in the pKO lines. **D**. Same as (B), for genotyping pAS insertions (left) and pEX clones (right). PCR was performed on the indicated cell lines using the primers listed in **Table S1**. **E.** Density plots of expression levels of the indicated genes in the indicated cell populations visualized through the ESpresso database [S5]. **F.** AP staining for the pluripotent state of pKO clones. **G.** Expression levels of *Meteor* in the indicated compartment of mESCs. Data taken from GEO dataset GSE99366. **H.** Predicted binding scores for TF binding sites (TFBS) defined in the JASPAR database [S6] in the WT and pInv sequence surrounding the *Meteor* TSS. The position of the TSS and the positions of the inversion breakpoints are shown by vertical lines. For each TFBS, the position with the highest score in the WT sequence is denoted by a black dot and shown at the position of the top-scoring hit in the WT sequence. For TFBSs for which the score in the inverted sequence is different, a gray point indicates the highest score in the inverted sequence, and the gray lines connect the scores in the WT and the inverted sequences. Scores below –20 were set to –20. Names of TFBSs for which the scores were below –20 in the inverted sequence are shown in gray. Scores for the pluripotency TFs and for EOMES are denoted in orange.

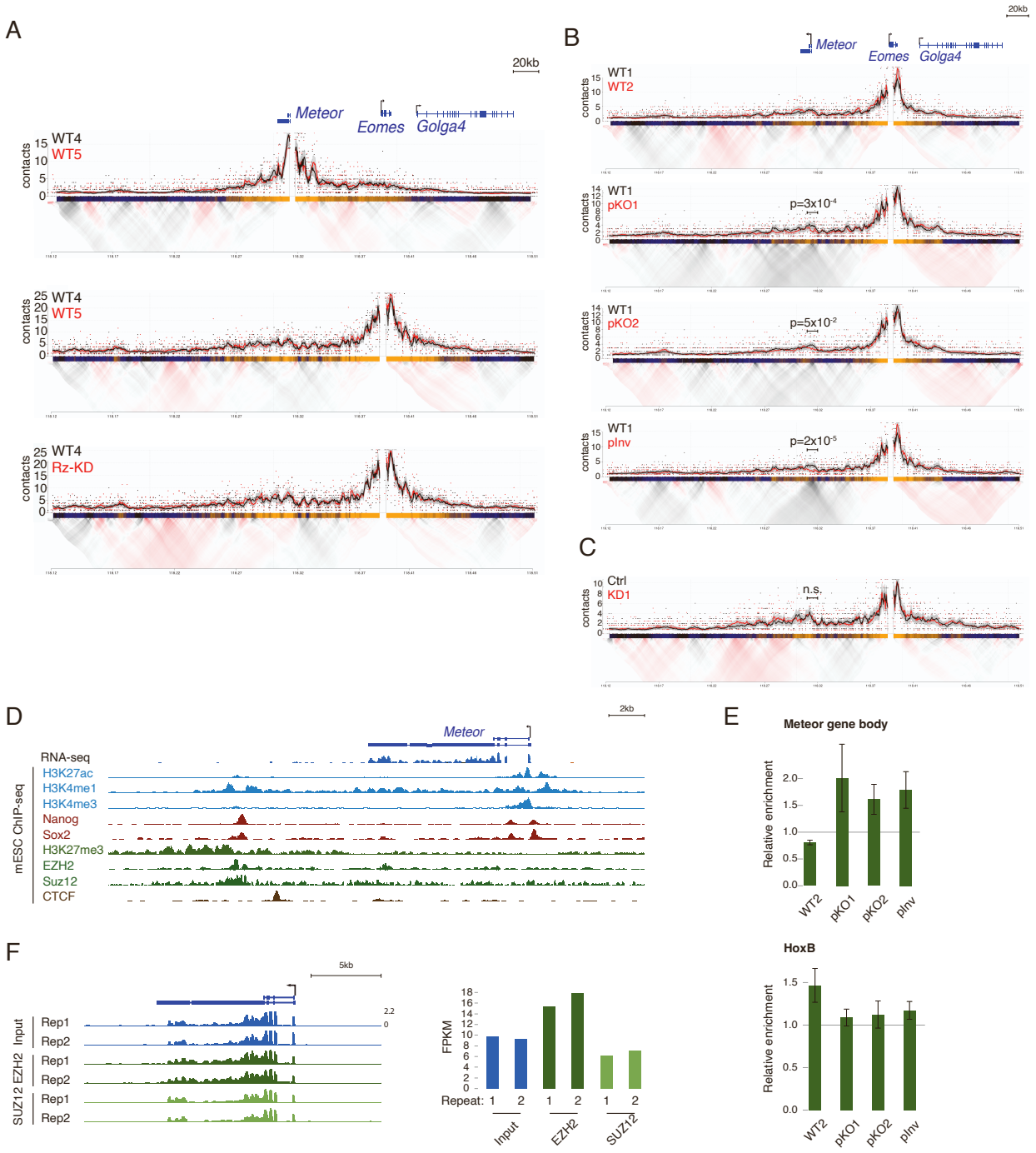

Figure S2. *Meteor* depletion induces chromatin changes in mESCs. Related to Figure 2.

A. 4C analysis in the indicated mESC lines using either the *Meteor* or *Eomes* promoters as viewpoints. Domainograms showing mean contact per fragment end for a series of window sizes are placed below smoothed trend lines and raw counts of the contact profiles. **B.** Same as (A), for *Meteor* pKO and pInv mESCs, using the *Eomes* promoter as the viewpoint. **C.** Same as (A), for *Meteor* KD mESCs, using the *Eomes* promoter as the viewpoint. **D.** Genome browser image of the *Meteor* locus. Shown are representative transcript models; RNA-seq tracks where orange denotes transcription on the plus strand

and blue denotes transcription on the minus strand; and mESC ChIP-seq tracks. **E.** Quantification of H3K27me3 Cut&Run levels in mESC lines grown in serum-free 2i/LIF conditions. Shown are H3K27me3 levels around the *Meteor* gene body, and at a control region around the *HoxB* locus. Signal was normalized to WT1 and to a H3K27me3-rich region near the *Ppib* gene (see **STAR Methods**). Bars represent standard errors; n=3. **F.** (Left) Genome browser shot of the *Meteor* locus, showing RNA immunoprecipitation (RIP) data of WT mESCs taken from [S7]. All tracks are normalized to the same scale. (Right) RSEM quantification of signal from the *Meteor* region in the same samples.

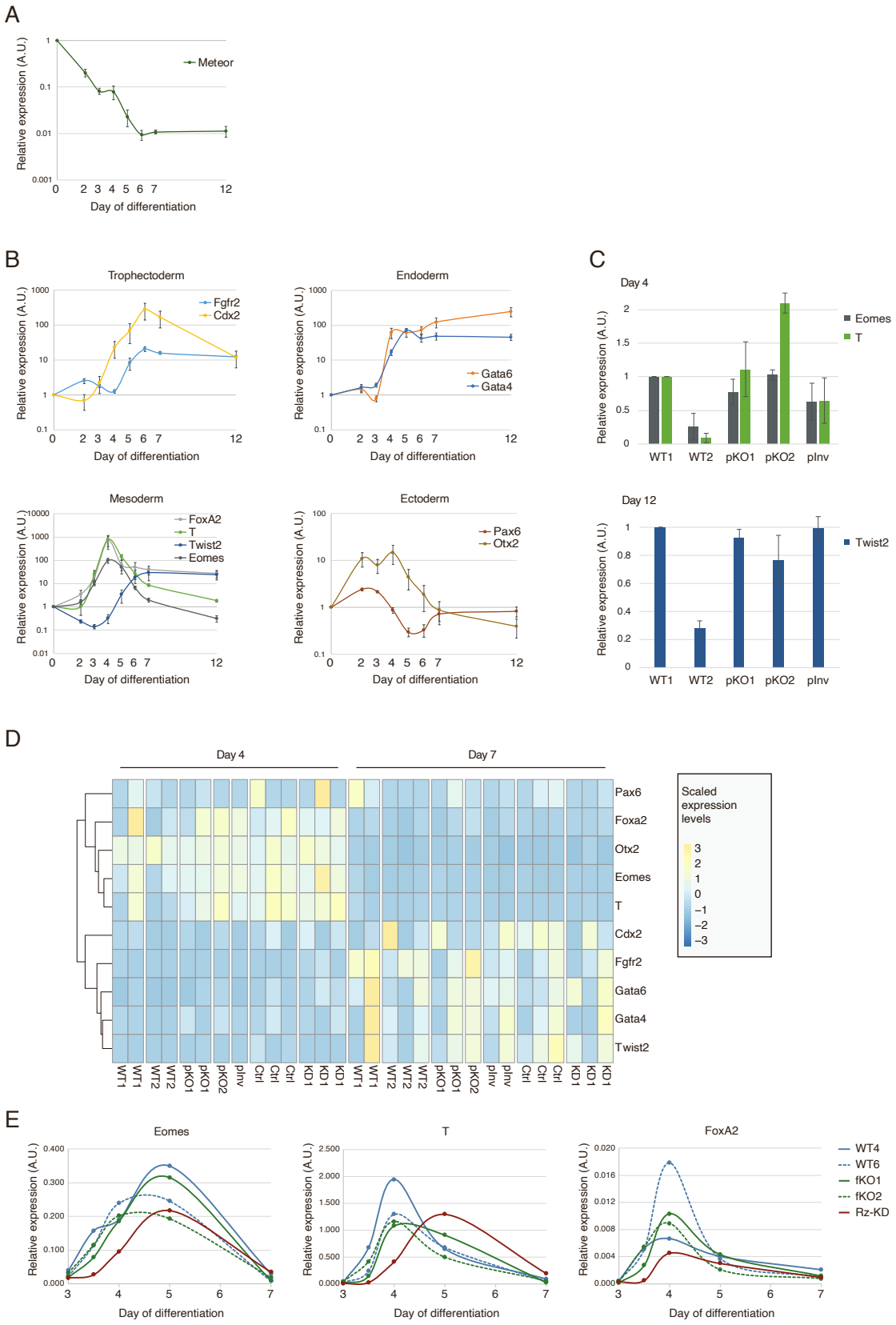
A
Meteor
Relative expression (A.U.)
Day of differentiation
B
Trophectoderm
Fgfr2
Cdx2
Endoderm
Gata6
Gata4
Mesoderm
FoxA2
T
Twist2
Eomes
Ectoderm
Pax6
Otx2
C
Day 4
Eomes
T
WT1
WT2
pKO1
pKO2
pInv
Day 12
Twist2
D
Day 4
Day 7
Pax6
Foxa2
Otx2
Eomes
T
Cdx2
Fgfr2
Gata6
Gata4
Twist2
Scaled expression levels
E
Eomes
T
FoxA2
WT4
WT6
fKO1
fKO2
Rz-KD

Figure S3. *Meteor* repression does not alter the cardiac mesoderm differentiation potential of mESCs. Related to Figure 3.

A. qRT-PCR quantifications of *Meteor* levels throughout EB differentiation. Levels were normalized to Sdha and to expression in mESCs (day 0). Bars represent standard errors; n=4. **B.** Same as (A), for the indicated markers of the different germ layers. **C.** qRT-PCR quantifications of the indicated mesoderm markers at day 4 (top) or day 12 (bottom) of EB differentiation of the indicated cell lines. Levels were normalized to Sdha. Bars represent standard errors; n=2. **D.** Heatmap of the scaled FPKM expression levels of the indicated genes in 3' RNA-seq data from the indicated day of EB differentiation. Each gene was scaled separately to mean 0 and standard deviation 1 across all the samples. **E.** qRT-PCR quantifications of the indicated markers at several time points throughout EB differentiation of the indicated cell lines. Levels were normalized to Sdha. n=2.

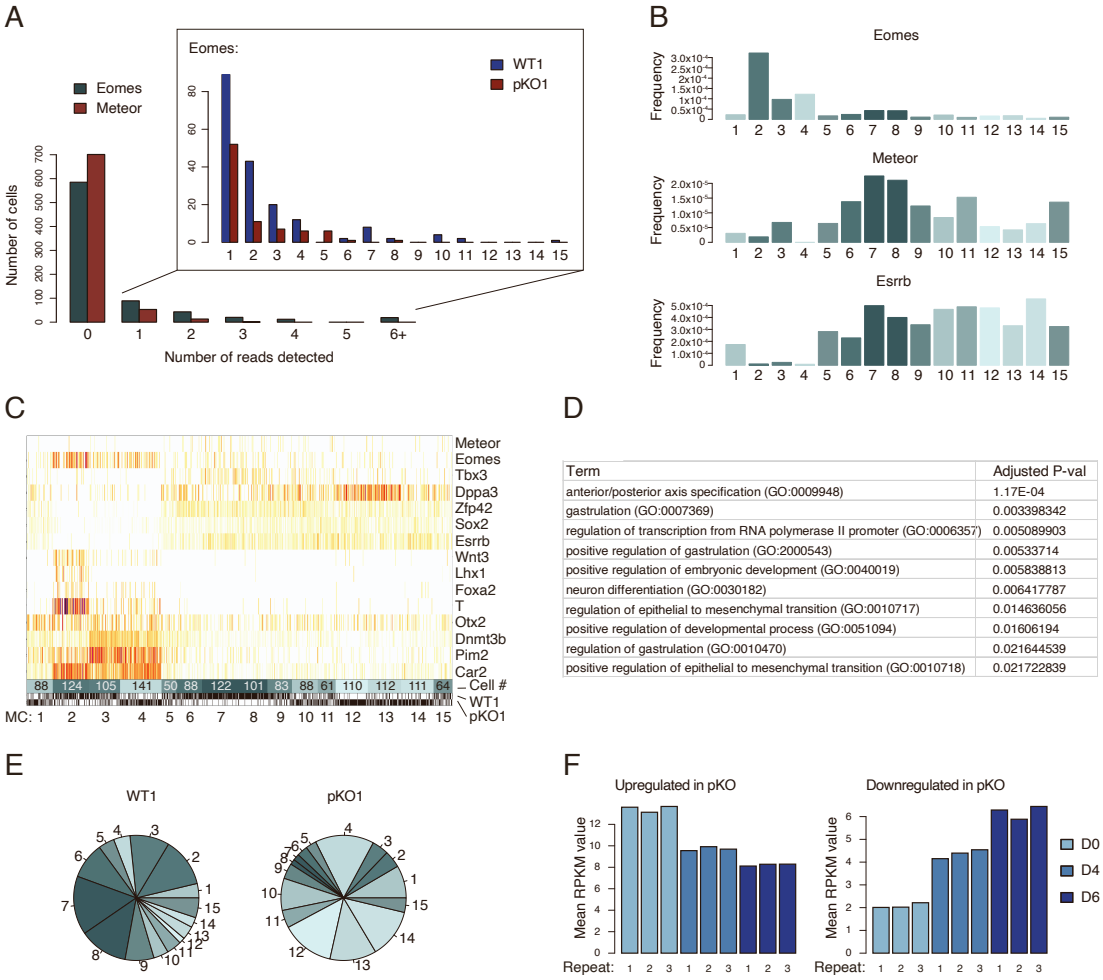

Figure S4. Single-cell RNA-seq of WT and *Meteor* pKO cells. Related to Figure 4.

A. Distribution of the number of unique reads per cell originating from the indicated transcript, for scRNA-seq of WT mESCs. Inset: same, for *Eomes* only, separately for WT and *Meteor* pKO cells, and showing only cells in which ≥1 *Eomes* reads were detected. **B.** Frequency of the indicated genes in each of the metacells (MCs). Color was assigned to each MC according to the ratio of WT and pKO cells that comprise it, with darker shades representing MCs comprised mostly of WT cells and lighter shades representing MCs comprised mostly of pKO cells. **C.** Heatmap showing enrichment values of the indicated key genes in individual cells (columns), grouped into MCs. Below: color assignments as in (B), overlayed with the number of cells in each MC; indication of the mESC line from which the cells originate; and MC number. **D.** GO terms associated with the 100 genes most highly correlated with *Eomes* in the scRNA-seq data. GO terms identified using Enrichr. **E.** Number of cells occupying the indicated MCs, separately for WT and pKO cells. Color assignments as in (B). **F.** Mean expression values of all the differentially regulated genes (FC ≥ 1.5 and padj < 0.05 in bulk RNA-seq of both *Meteor* pKO1 and pKO2), separately for upregulated (left) and downregulated (right) genes, in different timepoints of a dataset of control mESCs undergoing neural differentiation taken from [S8]. D0: pluripotent mESCs; D4: multipotent progenitors; D6: early neural progenitors.

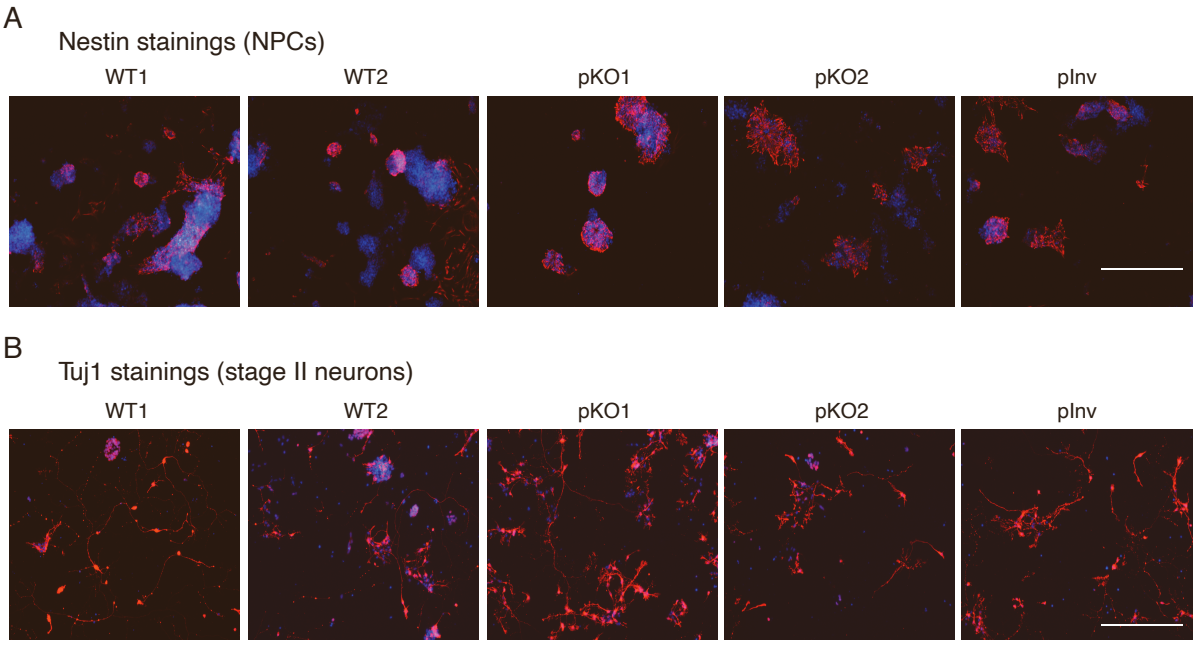

Figure S5. Neuronal differentiation of WT and *Meteor*-depleted cell lines. Related to Figure 5.

A. Nestin (red) stainings in NPCs derived from the indicated cell lines. Blue shows DAPI-colored nuclei. Scale bar = 400 µm. **B.** Same as (A), for Tuj1 (red) stainings in stage II neurons.

Table S1. Sequences of oligonucleotide used in this study, related to STAR Methods.

Purpose	Name	Sequence
4C of *Meteor* promoter	Upstream primer	tggggtccgaggcagagaacgcga
	Downstream primer	aatgatacggcgaccaccgagatctacactctttccctacacga cgctcttccgatctagagacagaagaagtcactatggc
4C of *Meteor* promoter in pKO mESCs	Upstream primer	tctaccagaagtgctaaagggatg
	Downstream primer	aatgatacggcgaccaccgagatctacactctttccctacacga cgctcttccgatctgtaatctataaagtgcttgcctata
4C of *Eomes* promoter	Upstream primer	ctacctgtgcaaccggcccctatg
	Downstream primer	aatgatacggcgaccaccgagatctacactctttccctacacga cgctcttccgatcttcaaattccaccggcaccaaactg
Meteor pKO	gRNA 1	aaaagctcggtagtaagagg
	gRNA 2	gccgtgaacattattcgggg
Meteor pKO genotyping	Primer A	aaattcgaggctggcactctgct
	Primer B	tgggcagataccaaccctct
	Primer C	agatgcccacagccaaaact
	Primer D	ggccaatcttgagtcttccgca
Meteor dCas9-KD	gRNA for KD1	gagctcacggacatgagg
	gRNA for KD2	gtccgaggcagagaacgcga
pAS cassette		tttgggggtcctaggcaggggcttccagaggtgcttggcactgct tggcacccctcccccgactcgattgtacgtgaagctccccctcc ccccgatcaagcacacaaaaaaccaacacacagatctaatgaa aataaagatcttttattcgggcagtaagtgtctcagctccattca gactgctgaccttggcatgggc
Meteor pAS genotyping	Forward primer	atccattgctcattcatttgca
	Reverse primer	tgggttatcgacagggaagt
Meteor PGK pEX cloning	*Meteor* Insertion F	gtaatacgactcactatagggcgaattggttggatttctgaccct cctg
	Meteor Insertion R	tgcttatgccatagtgacttcttctgtctcgcccgccgcgcgcttc g
	Hygromycin F	gagctcggttcccaggcttgggcatgaaaaagcctgaactcacc
	Hygromycin R	tccttcgcgttctctgcctcggccatagagcccaccgcat
	PGK F	ccgaggcagagaacgcgaaggaaggggtaggggagg
	PGK R	tagtgacttcttctgtctcgaaaggcccggagatgagg
Meteor PGK pEX	gRNA pEX	caagcctgggaaccgagctc
Meteor pEX genotyping	Forward primer	atacgaggtcgccaacatct
	Reverse primer	cttgggaaaagcgcctcccc
qRT-PCR of *Meteor*	Forward primer	aggactggcctgctagagaa
	Reverse primer	agtcagacagagcatccatcc

qRT-PCR of *Eomes*	Forward primer	tgtgacggcctaccaaaaca
	Reverse primer	tctgatgggatgaatcgtagttgt
qRT-PCR of *Fgfr2*	Forward primer	aaagaccacaaatgggcgac
	Reverse primer	ccacattaacaccccgaagga
qRT-PCR of *Cdx2*	Forward primer	gcggctggagctggagaaggagtt
	Reverse primer	cggcggctgtggaggctgttgt
qRT-PCR of *Gata4*	Forward primer	agctccatgtcccagacattc
	Reverse primer	agatgcatagccttgtgggg
qRT-PCR of *Gata6*	Forward primer	gacggcaccggtcattacc
	Reverse primer	acagttggcacaggacagtcc
qRT-PCR of *FoxA2*	Forward primer	ggagcccgagggctactct
	Reverse primer	gagcccgcgctcatgtt
qRT-PCR of *T*	Forward primer	gctctaaggaaccaccggtcatc
	Reverse primer	atgggactgcagcatggacag
qRT-PCR of *Twist2*	Forward primer	gtctcagctacgccttctcc
	Reverse primer	caggtgggtcctggcttg
qRT-PCR of *Pax6*	Forward primer	gggaccacttcaacaggact
	Reverse primer	cgaggccagtactgagacat
qRT-PCR of *Otx2*	Forward primer	aagacccggtacccagacatc
	Reverse primer	ttggcggcacttagctcttc
qRT-PCR of *Sdha*	Forward primer	gctcctgcctctgtggttga
	Reverse primer	agcaacaccgatgagcctg
qRT-PCR of *Ppib*	Forward primer	tgatccagggtggagacttc
	Reverse primer	attggtgtctttgcctgcat

References

[S1] Tuck AC, Natarajan KN, Rice GM, Borawski J, Mohn F, Rankova A, et al. Distinctive features of lincRNA gene expression suggest widespread RNA-independent functions. Life Sci Alliance 2018;1:e201800124.

[S2] Engreitz JM, Haines JE, Perez EM, Munson G, Chen J, Kane M, et al. Local regulation of gene expression by lncRNA promoters, transcription and splicing. Nature 2016;539:452–5.

[S3] Alexanian M, Maric D, Jenkinson SP, Mina M, Friedman CE, Ting C-C, et al. A transcribed enhancer dictates mesendoderm specification in pluripotency. Nat Commun 2017;8:1806.

[S4] Guo X, Xu Y, Wang Z, Wu Y, Chen J, Wang G, et al. A Linc1405/Eomes Complex Promotes Cardiac Mesoderm Specification and Cardiogenesis. Cell Stem Cell 2018;22:893–908.e6.

[S5] Kolodziejczyk AA, Kim JK, Tsang JCH, Ilicic T, Henriksson J, Natarajan KN, et al. Single Cell RNA-Sequencing of Pluripotent States Unlocks Modular Transcriptional Variation. Cell Stem Cell 2015;17:471–85.

[S6] Castro-Mondragon JA, Riudavets-Puig R, Rauluseviciute I, Berhanu Lemma R, Turchi L, Blanc-Mathieu R, et al. JASPAR 2022: the 9th release of the open-access database of transcription factor binding profiles. Nucleic Acids Res 2022;50:D165–73.

[S7] Garland W, Comet I, Wu M, Radzisheuskaya A, Rib L, Vitting-Seerup K, et al. A Functional Link between Nuclear RNA Decay and Transcriptional Control Mediated by the Polycomb Repressive Complex 2. Cell Rep 2019;29:1800–11.e6.

[S8] Stryjewska A, Dries R, Pieters T, Verstappen G, Conidi A, Coddens K, et al. Zeb2 Regulates Cell Fate at the Exit from Epiblast State in Mouse Embryonic Stem Cells. Stem Cells 2017;35:611–25.